

Article

Comparative Genomics Reveal the Utilization Ability of Variable Carbohydrates as Key Genetic Features of *Listeria* Pathogens in Their Pathogenic Lifestyles

Qunfeng Lu^{1,2,†}, Xiaoying Zhu^{3,4,5,†}, Qinqin Long^{4,5}, Xueli Yi⁶, Anni Yang^{1,2}, Xidai Long^{4,5,*} and Demin Cao^{4,5,*}

- ¹ Modern Industrial College of Biomedicine and Great Health, Youjiang Medical University for Nationalities, Baise 533000, China
² School of Medical Laboratory Sciences, Youjiang Medical University for Nationalities, Baise 533000, China
³ Medical College, Guangxi University, Nanning 530004, China
⁴ Clinical Pathological Diagnosis & Research Center, The Affiliated Hospital of Youjiang Medical University for Nationalities, Baise 533000, China
⁵ Department of Tumor Pathology, The Key Laboratory of Molecular Pathology (Hepatobiliary Diseases) of Guangxi, Baise 533000, China
⁶ Center for Clinical Laboratory Diagnosis and Research, The Affiliated Hospital of Youjiang Medical University for Nationalities, Baise 533000, China
* Correspondence: sjtulongxd@ymun.edu.cn (X.L.); caodm@ymun.edu.cn (D.C.)
† These authors contributed equally to this work.



Citation: Lu, Q.; Zhu, X.; Long, Q.; Yi, X.; Yang, A.; Long, X.; Cao, D. Comparative Genomics Reveal the Utilization Ability of Variable Carbohydrates as Key Genetic Features of *Listeria* Pathogens in Their Pathogenic Lifestyles. *Pathogens* **2022**, *11*, 1430. <https://doi.org/10.3390/pathogens11121430>

Academic Editors: Yasser Sanad, Steven Foley and Mohamed K. Fakhr

Received: 10 October 2022

Accepted: 23 November 2022

Published: 28 November 2022

Publisher's Note: MDPI stays neutral with regard to jurisdictional claims in published maps and institutional affiliations.



Copyright: © 2022 by the authors. Licensee MDPI, Basel, Switzerland. This article is an open access article distributed under the terms and conditions of the Creative Commons Attribution (CC BY) license (<https://creativecommons.org/licenses/by/4.0/>).

Abstract: Background: *L. monocytogenes* and *L. ivanovii*, the only two pathogens of *Listeria*, can survive in various environments, having different pathogenic characteristics. However, the genetic basis of their excellent adaptability and differences in pathogenicity has still not been completely elucidated. Methods: We performed a comparative genomic analysis based on 275 *L. monocytogenes*, 10 *L. ivanovii*, and 22 non-pathogenic *Listeria* strains. Results: Core/pan-genome analysis revealed that 975 gene families were conserved in all the studied strains. Additionally, 204, 242, and 756 gene families existed uniquely in *L. monocytogenes*, *L. ivanovii*, and both, respectively. Functional annotation partially verified that these unique gene families were closely related to their adaptability and pathogenicity. Moreover, the protein–protein interaction (PPI) network analysis of these unique gene sets showed that plenty of carbohydrate transport systems and energy metabolism enzymes were clustered in the networks. Interestingly, ethanolamine-metabolic-process-related proteins were significantly enriched in the PPI network of the unique genes of the *Listeria* pathogens, which can be understood as a determining factor of their pathogenicity. Conclusions: The utilization capacity of multiple carbon sources of *Listeria* pathogens, especially ethanolamine, is the key genetic basis for their ability to adapt to various environments and pathogenic lifestyles.

Keywords: *Listeria monocytogenes*; comparative genome; unique genetic composition; pathogenesis

1. Introduction

Listeria spp. are Gram-positive, rod-shaped, and facultative anaerobes that survive in various environments and are relatively resistant to environmental stress, such as low temperatures and low pH and high salt concentrations [1]. Currently, there are 30 identified species in the *Listeria* genus that are recorded in the List of Prokaryotic names with Standing in Nomenclature database (LPSN, <https://www.bacterio.net/genus/listeria>, accessed on 19 March 2022). Among them, *Listeria monocytogenes* and *Listeria ivanovii* are typical facultative intracellular parasites and are pathogenic to humans and ruminants, respectively. *L. monocytogenes* is the most prevalent species of the *Listeria* genus and an important food-borne pathogen. It is a great threat to people with low immunity, such as children, elderly individuals, pregnant women, and immunocompromised individuals [2,3]. *L. ivanovii* can

cause septicemic disease with enteritis, neonatal sepsis, and abortion in small ruminants and cattle [4]. Additionally, human cases of diseases caused by *L. ivanovii* are very rare. The other 28 *Listeria* spp., such as *L. grayi*, *L. marthii*, and *L. innocua*, are rarely reported to be pathogenic.

The pathogenicity of bacteria and their unique ability to adapt to their habitats have a distinctive genetic basis. Numerous relationships between genes and pathogenic phenotypes have been identified and studied in *L. monocytogenes* and *L. ivanovii* [5]. For example, *Listeria* pathogenicity island 1 (LPI-1) is a ~9 Kb region that consists of three operons essential for the intracellular parasitism of two *Listeria* pathogens [4]. The central position is *hly* monocistron that encodes listeriolysin O, a pore-forming toxin, which is required for the disruption of the phagocytic vacuole [6]. Upstream from *hly* lies the *plcA-prfA* operon. The *PlcA* is a phospholipase C with phosphatidylinositol activity, and *PrfA* is a virulence regulator [7,8]. Downstream from *hly* is a lecithinase operon that consists of three genes: *mpl*, *actA*, and *plcB*. The *actA* encodes a surface protein ActA that recruits and polymerizes actin monomers to promote cell-to-cell spreading [9]. The *plcB* encodes a phospholipase C with lecithinase activity, which is secreted as an inactive propeptide and extracellularly processed into the mature form by the *Mpl* protease [9,10]. However, the genetic basis of the pathogenicity and environmental adaptability of *Listeria* pathogens is incompletely understood and requires further elucidation.

In recent years, with the large-scale application of next-generation sequence and third-generation-sequence technology, numerous *Listeria* genomes have been sequenced and shared. The comparative genomic analysis of *Listeria* pathogens and non-pathogenic genomes could improve our understanding of the genetic mechanisms they use to adapt to diverse environments and their pathogenic lifestyles, which may further promote the diagnosis and treatment of *listeria* infections. The purpose of this study was to identify the genetic composition unique to the pathogenic *Listeria* species and to illustrate their role and the crucial functional gene clusters involved in their pathogenic lifestyle. Thus, we performed a comparative genome study of *L. monocytogenes* (LMO), *L. ivanovii* (LIV), and non-pathogenic *Listeria* spp. (NPLS). The core pan-genome of each *Listeria* group was analyzed, and the unique gene families of each group were acquired. Through functional annotation, functional enrichment analysis, and protein–protein interaction analysis, we identified the roles of these unique genes in each group in their pathogenicity and environmental adaptability. Meanwhile, the other genes with ambiguous functions could be used as candidate genes, which may be associated with their pathogenicity and environmental adaptation, for further investigation in the future. Finally, the antibiotic resistance genes, CRISPR-Cas systems, and plasmids of each *Listeria* species were investigated.

2. Materials and Methods

2.1. Data Retrieval and Management

In this study, we retrieved all the complete *Listeria* spp. genomes from the National Center for Biotechnology Information (NCBI) genome database (<https://www.ncbi.nlm.nih.gov/genome/?term=Listeria>, accessed on 19 March 2022). A total of 307 genomes were acquired, including 275 *L. monocytogenes*, 10 *L. ivanovii*, 8 *L. innocua*, 5 *L. seeligeri*, 4 *L. grayi*, 3 *L. marthii*, and 2 *L. welshimeri* complete genomes.

To avoid the contradictions caused by different gene prediction tools applied to the different datasets, Prodigal V2.6.3 [11] was used as the unique tool to predict the open reading frames (ORFs) for all the genomes. The rnammer 1.2 [12] tool was used to predict the rRNA genes, and tRNAscan-SE 2.0.9 [13] was used to predict the tRNA genes. The plasmid of each *Listeria* genome was detected with plasmidfinder 2.1.6.1 [14] and validated using the plasmid database v. 2021_06_23_v2 [15]. The details of the studied genomes, such as the accession number, genome size, GC content, number of genes, and so on, are summarized in Table 1 and listed in Table S1.

Table 1. Characteristics of *Listeria* species used in the study.

Species	Number of Genomes	Genome Size (bp) ¹	GC Content (%) ¹	Number of Scaffolds	Number of Plasmids	CDS ^{1,2}	rRNA ¹	tRNA ¹	Isolation Source
<i>L. grayi</i>	4	2,600,550 (2,598,321, 2,751,104)	41.52 (41.47, 41.73)	1–4	0–1	2609 (2561, 2982)	12 (7, 18)	58 (52, 65)	Homo sapiens, Plant
<i>L. innocua</i>	8	3,019,705 (2,889,727, 3,115,943)	37.38 (34.65, 37.48)	1	0–1	2934 (2622, 3130)	18 (0, 18)	67 (24, 67)	Food, Meat, Environment
<i>L. ivanovii</i>	10	2,924,216 (2,893,311, 3,133,385)	37.11 (34.59, 37.15)	1	0	2808 (2682, 2924)	18 (1, 18)	67 (27, 67)	Food, Sheep
<i>L. marthii</i>	3	2,884,551 (2,840,389, 2,947,729)	38.62 (36.79, 38.74)	1	0	2759 (2597, 2863)	18 (2, 18)	67 (28, 67)	Environment
<i>L. monocytogenes</i>	275	2,964,472 (2,776,517, 3,243,301)	37.98 (37.74, 38.29)	1	0–1	2906 (2730, 3323)	18 (4, 20)	67 (49, 72)	Cow, Chicken, Food, Homo sapiens, Pig, Goat, Meat, Horse, Rabbit, Environment
<i>L. seeligeri</i>	5	2,927,941 (2,797,636, 3,140,155)	37.30 (35.17, 37.38)	1	0–1	2779 (2590, 2846)	8 (1, 18)	63 (24, 67)	Environment
<i>L. welshimeri</i>	2	2,814,134 (2,814,130, 2,814,137)	36.35 (36.35, 36.35)	1	0	2,780 (2778, 2781)	18 (18, 18)	66 (66, 66)	Food
Total	295	2,959,738 (2,598,321, 3,243,301)	37.97 (34.59, 41.73)	1–4	0–1	2902 (2561, 3323)	18 (0, 20)	67 (24, 72)	-

Note: ¹ Median (Range). ² CDS, coding sequence.

2.2. Protein Orthologous Group Analysis

To decrease the complexity of the analysis, CD-HIT version 4.8.1 was used to identify the consistency sequence with the parameters “-c 0.99 -aL 0.99 -aS 0.99 -uL 0.01 -uS 0.01 -g 1”, and a representative sequence dataset was generated first [16]. Orthologous group analysis was conducted with the software OrthoMCL version 2.0.9 [17]. In short, the representative sequences of each amino acid sequence cluster were subjected to all-against-all Blastp comparisons to build a similarity matrix with an E-value cutoff of 1×10^{-5} and a coverage cutoff of 50%. Then, the Markov clustering algorithm (MCL) [18] was used to group the sequences. Finally, the grouped gene families were combined with the results of the CD-HIT clusters with a Python script. The percentages of orthologous protein between/inner genomes were calculated and visualized with a heatmap.

2.3. Phylogenetic Analysis

To investigate the phylogenetic relationships between the 307 *Listeria* strains, all the core single-copy proteins were extracted and aligned using MAFFT v7.490 [19]. Then, the aligned sequences were concatenated for each strain with a uniform gene order, and GBLOCKS 0.91b was utilized to remove the poorly aligned positions and divergent regions [20]. RAxML version 8.2.12 was used to compute the maximum likelihood (ML) phylogenetic tree using the 100 bootstrap repetitions approach [21]. The online tool Interactive Tree of Life (iTOL) v5 (<https://itol.embl.de>, accessed on 9 September 2022) was used to visualize the tree with midpoint rooting, and the collection time, geographic location, and the number of plasmid of each strain were annotated on the tree [22].

2.4. Estimation of Core and Pan-Genome Sizes

Based on the results of the protein orthologous group analysis, we estimated the core and pan-genome sizes of LMO, LIV, NPLS, and all the *Listeria* strains. Formulas (1) and (2) were used to fit the curves and describe the characteristics of the core and pan-genomes of each group, respectively. Specifically, 100 random permutation lists of all the strains for each strain group were calculated, and the median values were used to fit the curve.

2.5. Functional Features of the Core and Accessory Genomes

For the core and accessory genome gene sets of each *Listeria* group, EggNOG v5.0 and the Clusters of Orthologous Groups database (COGs, 2020 update, <https://www.ncbi.nlm.nih.gov/research/cog/>, accessed on 9 September 2022) were used to perform the functional annotation and categorization, and the results were integrated [23,24]. The percentage of each COG function category of each *Listeria* group gene set was shown in a bar chart. Moreover, the Virulence Factor Database (VFDB), TrEMBL, and InterProScan were used to predict the functions of the genes and served as a complement to the annotation [25,26].

2.6. Unique Gene Analyses of *L. monocytogenes* and *L. ivanovii*

Based on the gene cluster analysis results, the unique genes of LMO, LIV, and NPLS were identified. Additionally, the clusters shared by the *Listeria* species and their combinations were discovered using a Python script. The statistical results were illustrated in a Venn diagram using VennDiagram v1.6.0 [27].

2.7. Protein–Protein Interaction Network Analysis of Unique Protein Sets

The Search Tool for the Retrieval of Interacting Genes/Proteins (STRING v10.5, <https://string-db.org/>, accessed on 9 September 2022) was used to build the protein–protein interaction network of the unique gene sets of LMO, LVI, and both, respectively [28]. Additionally, the networks were visualized using Cytoscape 3.9.1 [29].

2.8. Antibiotic Resistance Gene Investigation of *Listeria* Genomes

The Resistance Gene Identifier (RGI-v6.0.1) was used for the detection of the antibiotic resistance genes of the 307 *Listeria* genomes based on the Comprehensive Antibiotic Resistance Database (CARD version 3.2.5) [30]. The results were summarized and shown in a heatmap using pheatmap version 1.0.12.

2.9. Identification of CRISPR–Cas Systems of *Listeria* Genomes

CRISPRCasFinder version 4.2.20 [31] was used for the detection and sub-typing of the Clustered Regularly Interspaced Short Palindromic Repeats and Cas genes (CRISPR–Cas) system of the 307 *Listeria* genomes. To obtain the functional CRISPR–Cas system, the presence of both the CRISPR sequence and Cas genes was considered as evidence for an actual CRISPR–Cas system and used for the further analysis.

3. Results and Discussion

3.1. Subsection

3.1.1. Genome Statistics and General Features

There are 30 identified species in the *Listeria* genus at present. *L. monocytogenes* EGD-e and *L. innocua* CLIP 11,262 were the first whole-genome-sequenced strains of the *Listeria* genus [32]. By searching the genome database of NCBI, we found 307 genomes of the *Listeria* genus at the complete genome level (Tables 1 and S1). Of those genomes, 275 of them belonged to LMO, the important food pathogens, and 10 of them were LVI, which is pathogenic mostly for ruminants. The other 22 genomes belonged to five NPLS species (eight *L. innocua*, five *L. seeligeri*, four *L. grayi*, three *L. marthii*, and two *L. welshimeri*). The median genome size of LMO was 2,964,472 (2,776,517~3,243,301) bp, and *L. monocytogenes* 1639 str2 had the largest genome size of all the genomes. *L. grayi* had the smallest genome size, with a median of 2,600,550 (2,598,321~2,751,104) bp. This genus had a low GC content,

with an average GC content of 37.97%, ranging from 34.59% (*L. ivanovii* FSL_F6_596_702454) to 41.73% (*L. grayi* 1641 str1). The median number of the ORF was 2902, ranging from 2561 (*L. grayi* DSM 20601) to 3323 (*L. monocytogenes* N53-1). One-fifth of them (18.54%, 51/275) had one plasmid. The LMO strains used in this study were isolated from various sources, including cow, chicken, food, *Homo sapiens*, pig, goat, meat, horse, rabbit, and the environment, indicating their excellent adaptive capacity to diverse environments.

3.1.2. Homologous Proteome Analysis and Phylogeny of the *Listeria* Genus

To estimate the similarity in the genetic make-up of the *Listeria* species, the percentages of the homologous proteome shared by each *Listeria* strain pair were calculated (Table S2), and the results are shown in Figure 1A. The percentages of homologous proteome between different *Listeria* species ranged from 92.45% (*L. innocua* 1642 vs. *L. monocytogenes* 1639 str194) to 61.45% (*L. grayi* 1641 str1 vs. *L. innocua* FSL_S4-378 702456), which suggested that *L. monocytogenes* and *L. innocua* had the closest relationship, while *L. grayi* had the greatest difference with *L. innocua* in terms of the proteome. Additionally, the percentage was higher than 85.00% between any two LMO strains. Compared with the proteome of the strains themselves, the percentage of homologous proteome ranged from 4.57% (*L. marthii* FSL_S4-120 702457) to 13.46% (*L. monocytogenes* 1639 v198). The high percentage of paralogous genes indicated that there were gene family expansion events in the LMO genomes, which are an important factor for bacteria that lead to changes in their biological capabilities and are associated with their host range [33].

It is medically interesting to note that the *Listeria* species survive in diverse habitats, but only LMO and LIV display pathogenicity. To understand the evolution pattern of *Listeria*, we performed a phylogenetic analysis of *Listeria* using the conserved amino acid sequences of 573 single-copy genes (Figure 1B). In consensus with the results of homologous proteome comparisons and previous studies, *L. grayi* showed the deepest branch within the genus [34]. The remaining six species formed two distinct groups with high bootstrap supports. One lineage contained *L. ivanovii* and *L. seeligeri*, while the other contained *L. welshimeri*, *L. innocua*, *L. marthii*, and *L. monocytogenes*. The pathogens LMO and LIV showed a longer evolutionary distance. The species closest to LMO were *L. innocua* and *L. marthii*, while the species closest to LIV was *L. seeligeri*. This topology structure is in agreement with the phylogenetic analysis results obtained by W. Schmid et al [35].

The collection period of the studied strains ranged from 1900 to 2021, and most of them were collected after 2002 (59.28%, 182/307, 77 strains without available collection dates) (Figure 1B (b)). About 1/4 of the strains were isolated from North American territories (USA, 76; Canada, 49), and 61 strains were isolated from different areas of Europe. Others came from Asia and Oceania or were without geographic information (Figure 1B (c)). There were 72 strains isolated from *Homo sapiens* and 64 strains isolated from the environment. Other isolation sources were food, meat, cattle, pig, sheep, and so on (Figure 1B (d)). The *Homo sapiens*-isolated LMO strains and others were uniformly spaced in the tree, which indicated their strong adaptive capacity to various environments of LMO strains.

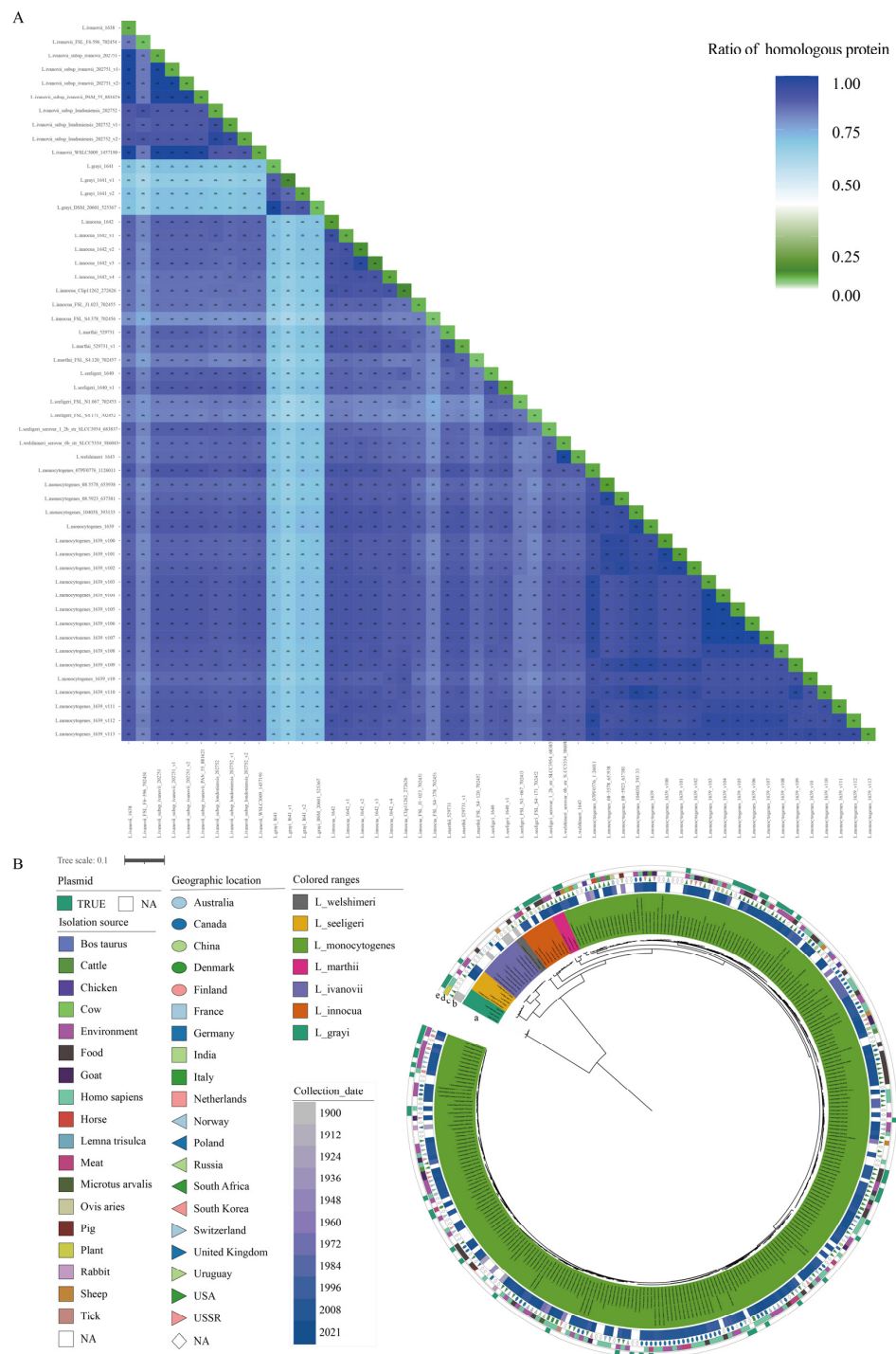


Figure 1. Homologous proteome analysis and phylogeny of the *Listeria* genus strains. **(A)** The percentages of homologous proteome among the *Listeria* strain pairs and within strains. The color depth of each block represents the percentage of the homologous proteome of the corresponding strain pairs. Twenty LMO genomes were selected as representatives in the heatmap. The number and percentage of the homologs between/within strains are presented in corresponding blocks. **(B)** Phylogenetic analysis of the *Listeria* strains examined in the present study. (a) The phylogenetic tree is based on the concatenated sequences of 573 single-copy core genes. The different species are shown in different colors. (b) The collection dates of the strains are shown in gradient colors. (c) The geographic locations of the strains isolated are shown with combinations of different shapes and colors. (d) The isolation sources of strain are shown in different colors. (e) The presence of plasmids in each strain is shown with a green color bar.

3.1.3. Core and Pan-Genome Sizes of *Listeria* Species

To assess the genome polymorphism of the *Listeria* species, we performed a core/pan-genome analysis. The core genome consists of the genes shared by all the studied strains and is essential to their basic lifestyles and major phenotypic traits [36]. The pan-genome is the total of the core genomes and accessory genomes that are only presented in some strains, as well as the genes unique to single strains [37]. The core genome size of 307 *Listeria* strains that belonged to seven different species was 975, nearly one-third of the average number of coding genes, and their pan-genome size was 7701, including 1867 singletons. For 275 LMO strains, the core and pan-genome sizes were 2060 and 5382, respectively. For 10 LIV strains, the core and pan-genome sizes were 2118 and 3194, respectively. For the other 22 NPLS strains, the core and pan-genome sizes were 1203 and 5833, respectively. In addition, we created a fit curve of the core and pan-genomes using the functions (a) and (b) of each *Listeria* group (Figure 1).

The Heaps' law model (function b) was used to fit the pan-genome size. The exponent size (B_1) indicates the attribute of the pan-genome. In detail, $0 \leq B_1 \leq 1$ indicates that the genome of the studied strains is open; otherwise, it is closed. As shown in Figure 2, the core genome size curve of each group tended to quickly converge, but their pan-genome size curves tended to dilate. Respectively, the fitting parameter B_1 of the pan-genome size curves of all the *Listeria* strains, LMO, and NPLS were 0.308, 0.201, and 0.273, which suggested that these three *Listeria* strain groups had open genomes (Figure 2A,B,D). Yet, due to the fact that only 10 LIV genomes were available, more samples are needed to estimate the attribute of the pan-genome in the future (Figure 2C). The accessory genome contributes to the diversity of the species and confers selection advantages, such as niche adaptation, antibiotic resistance, and pathogenic ability [36–38]. The open genome and fertility of the accessory genome provide the hereditary foundation required for the *Listeria* species to survive in various environments.

3.1.4. Functional Features of the *Listeria* Core and Accessory Genomes

It is generally believed that the core genome represents the elemental parts that are necessary for the existence and shared phenotypic characteristics of given strains. The accessory genome provides the unique characteristics of a species or a strain, which is not indispensable for their basic life but provides selective advantages for niche adaptation and drug resistance [37]. In this study, the core and accessory genome sizes of all the studied *Listeria* strains, LMO, LIV, and NPLS were 975/6726, 2006/3376, 2118/1076, and 1203/4630, respectively. According to the COG and EggNOG annotations, the gene sets of the core and accessory genomes of each strain group were divided into 22 different functional sub-categories (Figure 3). Additionally, the unannotated genes were assigned to the "Function unknown" category.

In line with our expectations, the top enriched categories of the core genomes of each gene family set were related to the basic life process. For the core genomes of all the *Listeria* strains, LMO, LIV and NPLS, the most enriched functional categories were (a) translation, ribosomal structure, and biogenesis (10.58%, 8.80%, 7.77, and 10.00%, respectively), (b) amino acid transport and metabolism (8.19%, 7.44%, 7.42%, and 8.28%, respectively), (c) transcription (7.73%, 7.76%, 8.15%, and 7.39, respectively), and (d) coenzyme transport and metabolism (6.62%, 6.26%, 5.52%, and 6.19%, respectively). These COG categories had a higher proportion of the core genomes rather than the accessory genomes of each strain group. Unlike the core genome, for the accessory genome of each group, the category of mobilome, including prophages and transposons (1.16% vs. 0.18%, 1.81% vs. 0.31%, 2.76% vs. 0.22%, and 2.19% vs. 0.15%, respectively), which is related to the acquisition of new pathotypes of bacteria [39], was found in a higher proportion than the core genome. However, more than 57.00% of the gene families of the accessory genome had no defined function information.

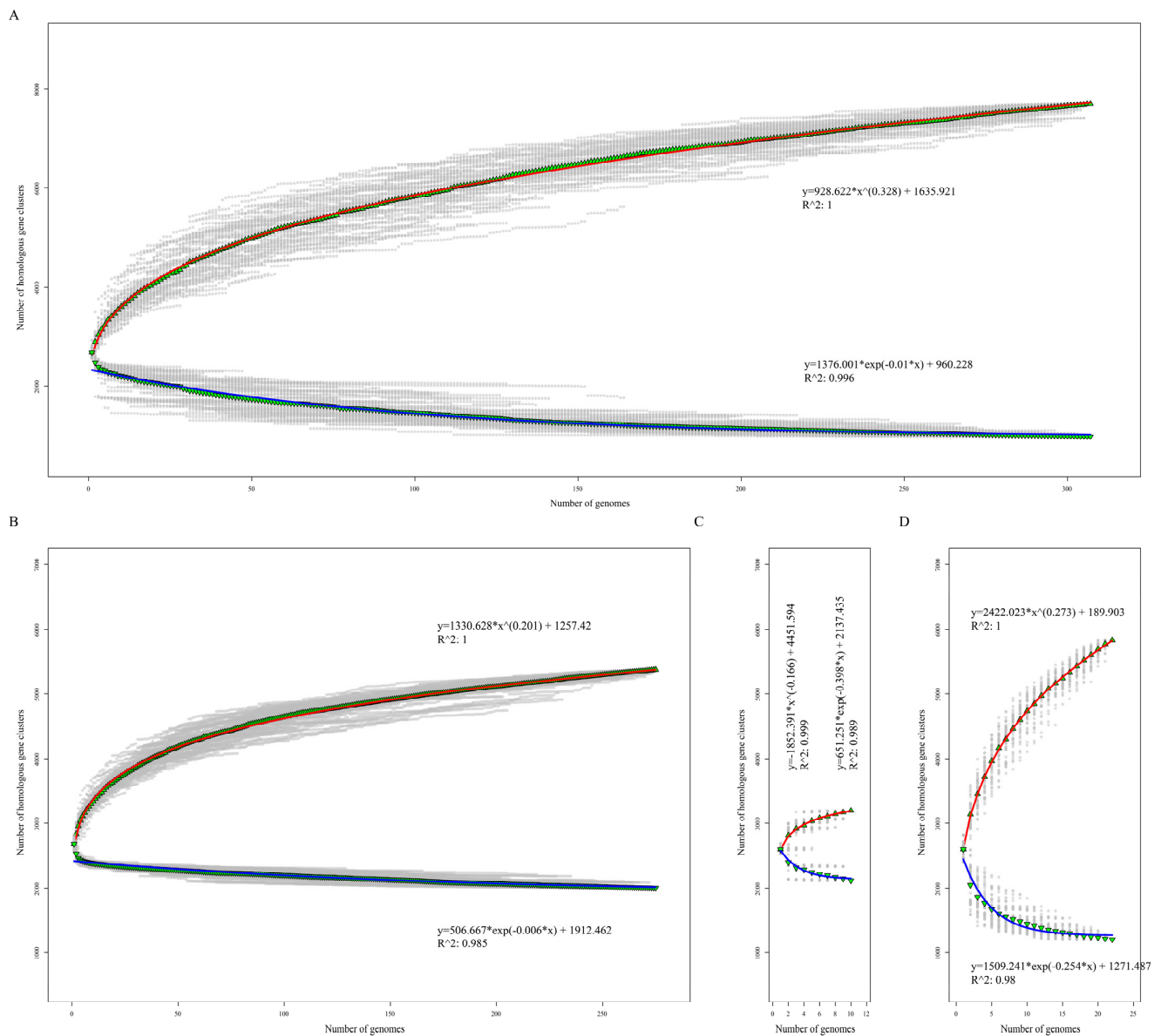


Figure 2. Core and pan-genome size evolution. Accumulation curves of the core and pan-genomes of 307 *Listeria* strains (A), 275 *L. monoeytogenes* (B), 10 *L. ivanovii* (C), and 22 non-pathogenic *Listeria* strains (D), respectively. Blue and red curves represent the core and pan-genome fitting curves of each group. The ▼ and ▲ represent the average core and pan-genome size of each group with 100 random permutations.

3.1.5. The Transport Systems for Carbohydrates and Ions Enriched in Unique Gene Set of *Listeria* Pathogens and Closely Related to Their Pathogenesis

It is a plausible hypothesis that the unique phenotypes of an organism have a unique genetic makeup as the basis for supporting its adaption to a unique and complicated environment [38]. As shown in Figure 4A, there were 975 gene families shared by all the 307 *Listeria* genomes, which is consistent with the results of the core genome analysis. It is interesting to note that as many as 756 (31.4%) gene families were unique gene families of *Listeria* pathogens (UGLP) that were shared by LMO and LIV but absent in NPLS. In addition, there were 204 unique gene families for LMO (UGLMO) and 242 unique gene families for LIV (UGLIV). These unique gene families of *Listeria* pathogens are the crucial elements that are responsible for their pathogenicity and niche adaptability. To verify our hypothesis, we investigated the gene functions of UGLP, UGLMO, and UGLIV using the COG, VFDB, and UniProt databases, respectively.

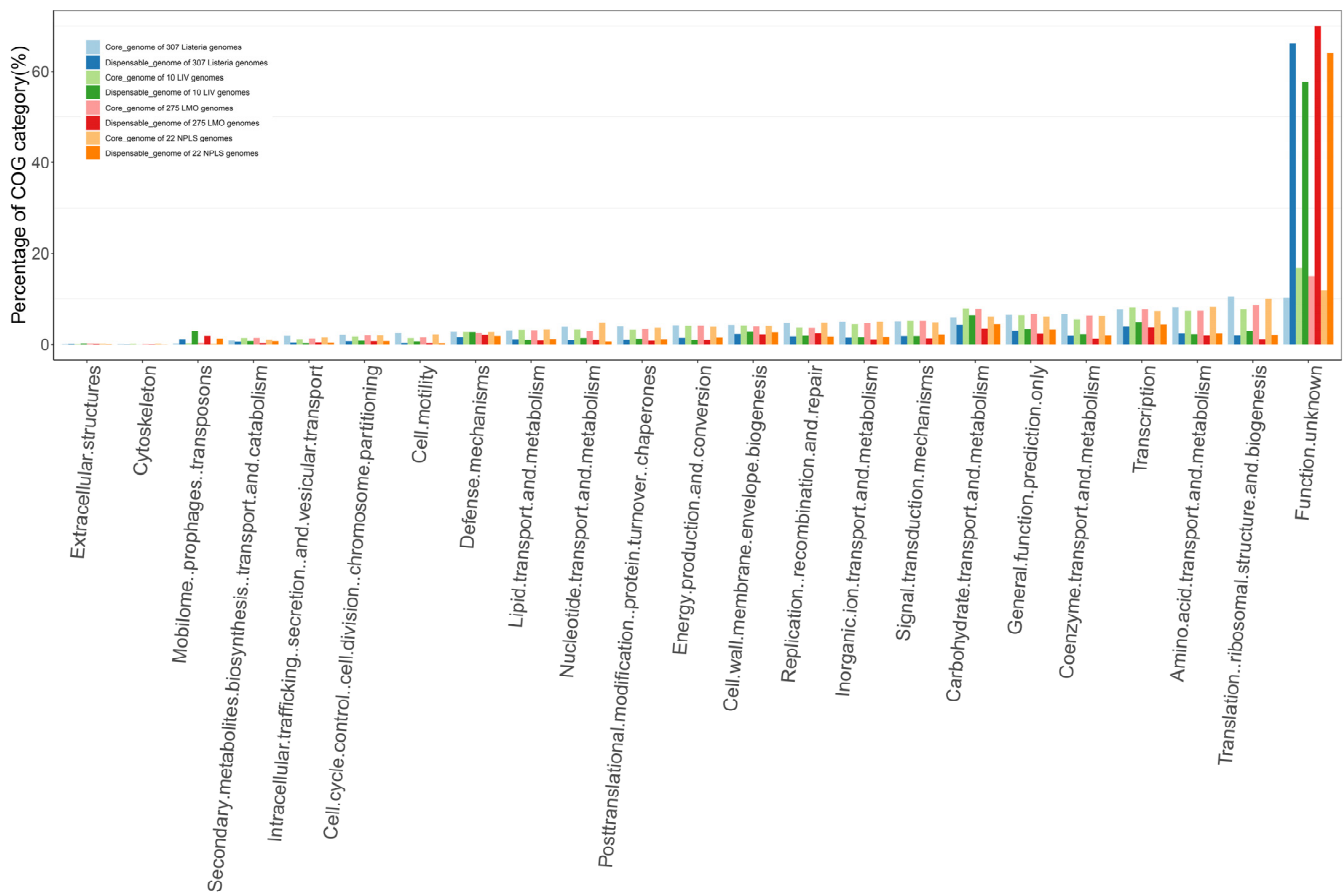


Figure 3. Function categories of the core and accessory genomes of each *Listeria* strain group in the COG and EggNOG databases. The COG categories of the core and accessory genomes of 307 *Listeria* genomes, 10 LIV genomes, 275 LMO genomes, and 22 NPLS genomes are shown in the graph with paired colors, respectively.

The two most enriched COG categories of UGLP (Figure 4B and Tables S5 and S6) were carbohydrate transport and metabolism (9.11%) and transcription (8.12%), which are related to the basic metabolism, and many of them have been proven to be important genes that affect the species' adaptability. A large number of transport systems for sugars and sugar derivatives, which were classified into two major types, ATP-binding cassette (ABC) transporters and the carbohydrate phosphotransferase system (PTS) (Table 2), were found in the UGLP gene set. Variable carbon source utilization is an important factor that influences the virulence gene expression of LMO and is related to the outbreak of listeriosis [40–42]. Most carbohydrates used by *Listeria* pathogens, including cellobiose, fructose, mannose, N-acetylgalactosamine, and sorbitol, are transported by PTS transporters [41]. However, the genes of fructose-specific PTS were considerably enriched in LMO compared to LIV (7 vs. 2), and the genes of mannitol- and galactitol-specific PTSs were only detected in the LMO strains. In addition, there were few genes of ABC transporters that are related to the metabolism of polysaccharide and glycerol-3-phosphate. The capability to metabolize a variety of carbon sources is important for expanding the range of the living niche. As shown in Figure 1B (c), LMO strains can survive in various environments, such as water, meat, markets, a variety of animals, and so on. Surviving in diverse environments may provide the various possible transmission routes for *Listeria* pathogens to infect humans and animals. Furthermore, many ABC transporters with other functions were found in the UGLP gene set (Table 2). Additionally, they were in charge of multidrug transport, ion transport, and so on, which play a vital role in *Listeria* pathogens' ability to survive inside and outside the host [43,44]. For example, disrupting *fur*, which is the regulated gene of

ferrous ABC transporters, resulted in a significant reduction in the virulence potential of LMO in mice, and the virulence defect could be rescued by overloading [45,46].

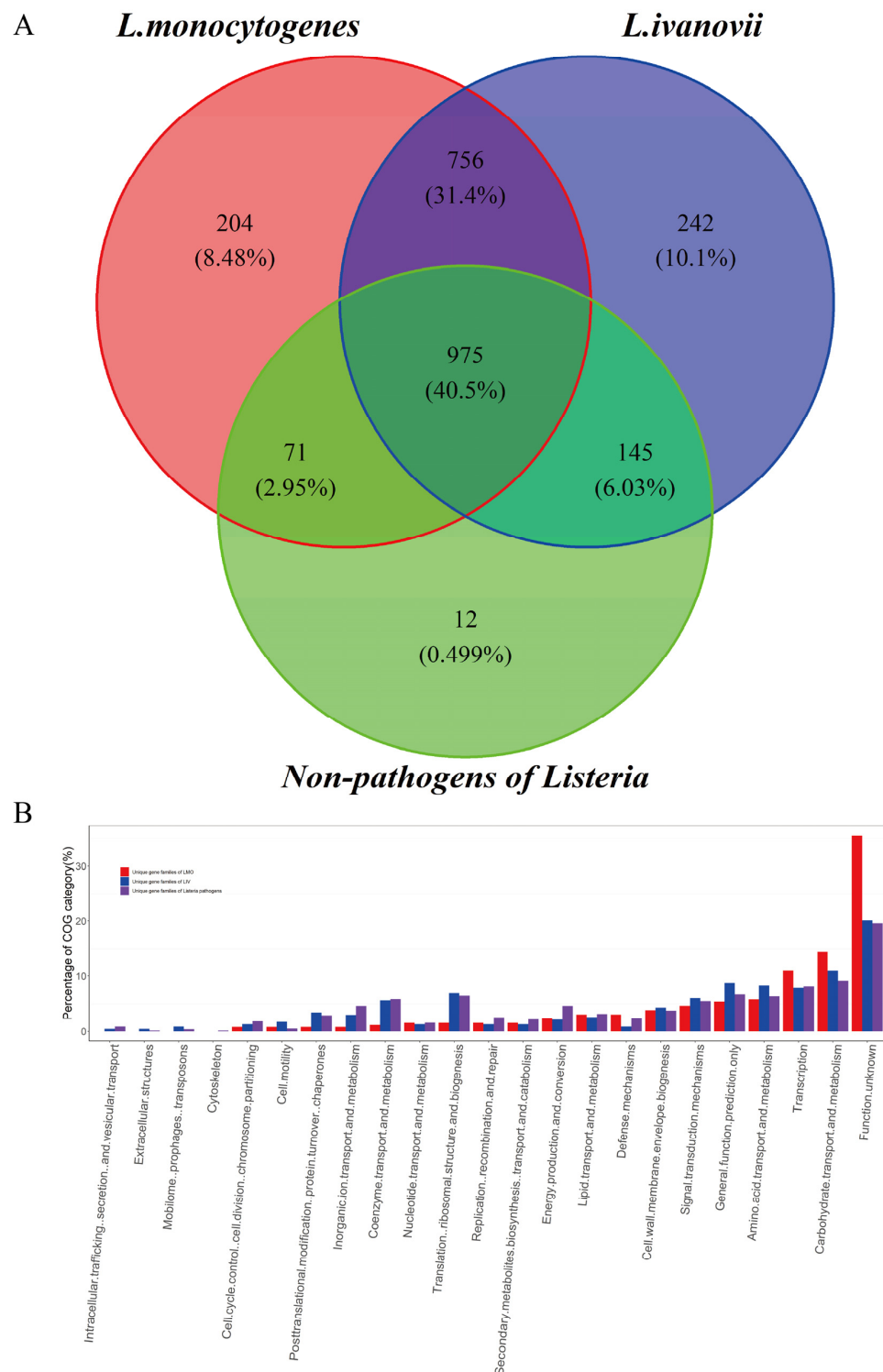


Figure 4. Function categories of the unique gene families of LMO, LIV, and both. **(A)** The Venn diagram for the gene sets of *L. monocytogenes*, *L. ivanovii*, and non-pathogens of *Listeria*. The number and proportion of the gene families are shown in the graph. **(B)** Function categories of the unique gene sets of LMO, LIV, and both according to the COG and EggNOG databases. The COG categories of 204 LMO unique genes, 242 LIV unique genes, and 756 genes that were shared by LMO and LIV but absent in NPLS are shown in the graph with different colors, respectively.

3.1.6. Virulence Factor Gene Investigation of the Unique Genes of *Listeria* Pathogens

To investigate the relationships between the unique genes of the *Listeria* pathogens and their pathogenesis, we performed virulence factor encoding genes annotation of the UGLMO, UGLIV, and UGLP gene sets, respectively. As listed in Table 3, there were 3 ORFs of UGLMO, 4 ORFs of UGLIV, and 18 ORFs of UGLP that could be annotated by VFDB (Tables 3 and S3–S6). They belonged to nine virulence-related function categories, such as invasion, adherence, immune modulation, exotoxin, and so forth.

The three virulence genes of the UGLMO were *prfA*, *actA*, and *aut*. The pleiotropic regulatory factor (PrfA) is known as the principal regulator of LIPI-1, which expresses PlcA, PlcB, ActA, and Mpl [47]. The assembly-inducing protein (ActA) is greatly induced in the host cytoplasm and activates the ARP2/3 complex to polymerize actin and spread the bacteria from one cell to another [48]. The surface protein Auto with autolytic activity encoded by *aut* is required for LMO's ability to enter into eukaryotic cells and necessary for its full virulence in vivo [49]. For the UGLIV, four virulence factor genes were identified, including the immune modulation genes internalin C (InlC), hexose phosphate transport protein (Hpt), sphingomyelinase-c (SmcL), and cytolysin regulator R2 (CylR2). The InlC protein can dampen the innate immune response and perturb the apical cell junctions, which promotes the cell-to-cell spread of *Listeria* [50,51]. The Hpt helps intracellular pathogens to exploit hexose phosphates from the host cell as a source of energy in order to promote bacteria growth within the cell. Its absence leads to the impaired intracellular growth of *listeria* and its reduced virulence in mice [52]. The SmcL mediates the membrane disruption of the phagosomes and the release of LIV into the cytosol [53].

It was noted that numerous adherence-, invasion-, and immune-modulation-related genes were shared by LMO and LIV, including *inlA*, *inlB*, *IlpA*, *ami*, *inlF*, *tufA*, *cps4I*, *gndA*, and *hasC*. They are critical genes that mediate *Listeria* pathogens' adherence to and entry into the host cells. For instance, the N-terminal 15 leucine-rich repeat (LRR) region of InlA interacts with the E-cadherin of the host cell surface protein, which promotes LMO entry into the host cell [54]. Autolysin amidase, the product of *ami*, interacts with the glycosaminoglycans of the host cell to promote efficient adhesion to, and colonization in, the mouse hepatocytes of LMO [55,56]. The InlF, which can bind to surface-localized vimentin, is essential for LMO's invasion of the host cell in brain infections [57]. Furthermore, four nutritional/metabolic factor genes (*mgtB*, *hbp1/svpA*, *hbp2*, *isdE*) and three exotoxin genes (*plcA*, *hly*, *plcB*) were detected in UGLP. It has been found that Hbp1 and Hbp2 are responsible for the acquisition of haem iron [58]. Specifically, Hbp1 can promote LMO's escape from the phagosomes of macrophages [59]. The exotoxin factor phospholipase C (PlcA) and lecithinase (PlcB) cooperate with listeriolysin O (Hly) to mediate the dissolution of the membranes of phagosomes and the bacteria's efficient escape to the cytoplasm [60,61]. Finally, exotoxin Mpl and the post-translational modification proteins GtcA and PrsA2 were found in the UGLP. Zinc metalloprotease (Mpl) is necessary for the maturation of PlcB [62]. The PrsA2 is a post-translocation chaperone, which mediates the secretion and maturation of the virulence proteins of *listeria* [63]. The glycosylation protein GtcA is involved in the modification of cell wall teichoic acid together with galactose and glucose and is related to cellular invasiveness [64].

Table 2. Unique transporter genes of *Listeria* pathogens.

Type of Transporter	Type of Substrate	Protein Name	ORFs ¹ (Referenced to <i>L. monocytogenes</i> EGD-e_169963)	ORFs (Referenced to <i>L. ivanovii</i> 1638)
Phosphotransferase system	cellobiose	CelC, CelA, CelB	orf_1724, orf_2698, orf_915, orf_2723, orf_916	orf_1158, orf_242, orf_2009, orf_186, orf_2008
	fructose	FrwB	orf_2144, orf_397, orf_425, orf_633	orf_2291, orf_722
		FrwC	orf_398, orf_426, orf_632	NE ²
	mannose/fructose/N-acetylgalactosamine	AgaB, ManY, ManZ, ManX	orf_2009, orf_22, orf_2008, orf_783, orf_96, orf_2007, orf_24, orf_782, orf_2004, orf_785	orf_2656, orf_869, orf_2151, orf_2780, orf_870, orf_2152, orf_871, orf_2149, orf_874
	sorbitol	SrlB, SrlE, SrlA,	orf_542, orf_543, orf_544	orf_2404, orf_2403, orf_2402
galactitol mannitol	SgaB MtlA	orf_1979, orf_2663 orf_2816	NE NE	
ABC-type transport system	sugar transport	MalK, UgpA	orf_2132, orf_2856, orf_861	orf_2613, orf_2068, orf_735, orf_75
	polysaccharide	LplB	orf_2016	orf_862
	glycerol-3-phosphate	UgpB	orf_2014, orf_2857, orf_860	orf_864
		UgpE	orf_2015, orf_2855	NE
	multidrug transport	MdlB, CcmA, YadH	orf_106, orf_1135, orf_2766, orf_607, orf_608, orf_2235, orf_980, orf_987, orf_981, orf_988	orf_143, orf_1807, orf_2332, orf_2333, orf_2767, orf_1934, orf_2207, orf_635, orf_1932, orf_1933, orf_2206
			orf_1040, orf_1207, orf_1208, orf_2192, orf_1964, orf_281, orf_1453, orf_1855, orf_1452, orf_1854, orf_1042, orf_1041, orf_1676, orf_2190	orf_1727, orf_1726, orf_678, orf_915, orf_2606, orf_1028, orf_1450, orf_1029, orf_1451, orf_1878, orf_1879, orf_1206, orf_680
	Mn ²⁺ / Zn ²⁺ / Fe ³⁺ / Co ²⁺ / Mo ²⁺	PotA, CbiM, CbiN, FepB, FepD, NlpA, ZnuC, ZnuB, ModA, ModB, ZnuA, FepC	orf1_192, orf1_2259, orf1_2358, orf1_1511, orf1_279, orf1_1227	orf1_2529, orf1_2703, orf1_611, orf1_2607, orf1_1393, orf1_2608, orf1_1700
antimicrobial peptide, polar amino acid, methionine, lipoprotein,	SalY, GlnQ, AbcC, LolD, MetP, LolC	orf1_133, orf1_1210, orf1_2731, orf1_920, orf1_745, orf1_1134	orf1_2004, orf1_2751, orf1_1724, orf1_2188, orf1_178, orf1_1808	
Others	EcfA2, DdpA, Uup, CcmA, CydD			

Note: ¹ ORFs, open reading frames. ² NE, not existing.

3.1.7. Ethanolamine-Metabolic-Related Proteins Enriched in the Protein–Protein Interaction Network of *Listeria* Pathogens' Unique Genes

The protein–protein interaction network plays an important role in accomplishing various kinds of vital movements in living organisms. To further assess the associations between the unique genes of the *Listeria* pathogens, we performed a PPI analysis of the UGLP, UGLMO, and UGLIV gene sets using STRING, respectively. There were 189 genes included in the UGLMO PPI network (Figure 5A, Table S3). They were clustered into a cluster, which indicated that they had strong associations in terms of their physical interactions or functional associations. Seventy-seven (77/189, 40.74%) of them were related to basic substance transport and metabolism, including six ABC-type transport system

proteins (orf_2359, orf_2360, orf_2361, orf_135, orf_862, orf_849) and fourteen PTS system proteins (orf_1978, orf_1979, orf_21, orf_23, orf_2662, orf_2663, orf_2664, orf_2814, orf_2816, orf_297, orf_396, orf_398, orf_426, orf_632), as well as numerous enzymes related to energy metabolism. Moreover, thirty-six of them were related to genetic information processing, including nine DNA-binding transcriptional regulators. These regulators control gene expression in a variety of metabolic processes in bacteria, enabling them to adapt to complex and changeable environments. For example, the deletion or over-expression of the multiple antibiotic resistance regulator (MarR) of *Chromobacterium violaceum* significantly changed the gene expression of the oxidative stress response (*ohrA/ohrR*), anaerobic nitrate respiration (*narK1K2* and *narGHJI*), and biofilm formation (*RTX*) [65]. Furthermore, twenty-one proteins in the network were related to cell wall/membrane/envelope biogenesis and cell motility. Three flagella-related proteins (orf_708, orf_1077, orf_2706) and two cell-wall-biosynthesis-related proteins (orf_933, orf_2562) were clustered together in the network. It has been proved that flagellar motility is critical for *L. monocytogenes* biofilm formation and host cell invasion [66,67].

Table 3. Unique virulence genes of *Listeria* pathogens.

Function Category	Gene Name	UGLMO ¹	UFLIV ²	UGLP(LMO) ¹	UGLP(LIV) ²	Gene's Description of VFDB
Regulation	<i>prfA</i>	orf1_197				Listeriolysin-positive regulatory protein
Motility	<i>actA</i>	orf1_201				Actin-assembly-inducing protein precursor
Invasion	<i>aut</i>	orf_1077				Autolysin
	<i>inlA</i>			orf_431	orf_2509	Internalin A
	<i>inlB</i>			orf_432	orf_2506	Internalin B
Immune modulation	<i>inlC</i>		orf_348			Internalin C
	<i>cps4I</i>			orf_2549	orf_401	Capsular polysaccharide biosynthesis protein Cps4I
	<i>gndA</i>			orf_1382	orf_1532	NADP-dependent phosphogluconate dehydrogenase
Nutritional/metabolic factor	<i>hasC</i>			orf_1079	orf_1839	UTP-glucose-1-phosphate uridylyltransferase
	<i>mgtB</i>			orf_2703	orf_239	Mg ²⁺ transport protein
	<i>hbp1/svpA</i>			orf_2194	orf_676	Haemoglobin-binding protein 1
	<i>hbp2</i>			orf_2193	orf_677	Hypothetical protein
	<i>isdE</i>			orf_2192	orf_678	Iron-regulated surface-determinant protein E
Exoenzyme	<i>hpt</i>		orf1_2093			Hexose phosphate transport protein
	<i>smcL</i>		orf1_1675			Sphingomyelinase-c
	<i>mpl</i>			orf_200	orf_2695	Zinc metalloproteinase precursor
Exotoxin	<i>cylR2</i>		orf1_2557			Cytolysin regulator R2
	<i>plcB</i>			orf_202	orf_2693	Phospholipase C
	<i>hly</i>			orf_199	orf_2696	Listeriolysin O precursor
Adherence	<i>plcA</i>			orf_198	orf_2697	Phosphatidylinositol-specific phospholipase c
	<i>tufA</i>			orf_2666	orf_278	Elongation factor Tu
	<i>ami</i>			orf_2570	orf_1680	Autolysin amidase, adhesin
Post-translational modification	<i>inlF</i>			orf_407	orf_474	Internalin F
	<i>gtcA</i>			orf_2561	orf_385	Wall teichoic acid glycosylation protein
	<i>prsA2</i>			orf_2227	orf_643	Post-translocation chaperone

Note: ¹ Referenced to *L. monocytogenes* EGD-e_169963; ² referenced to *L. ivanovii* 1638.

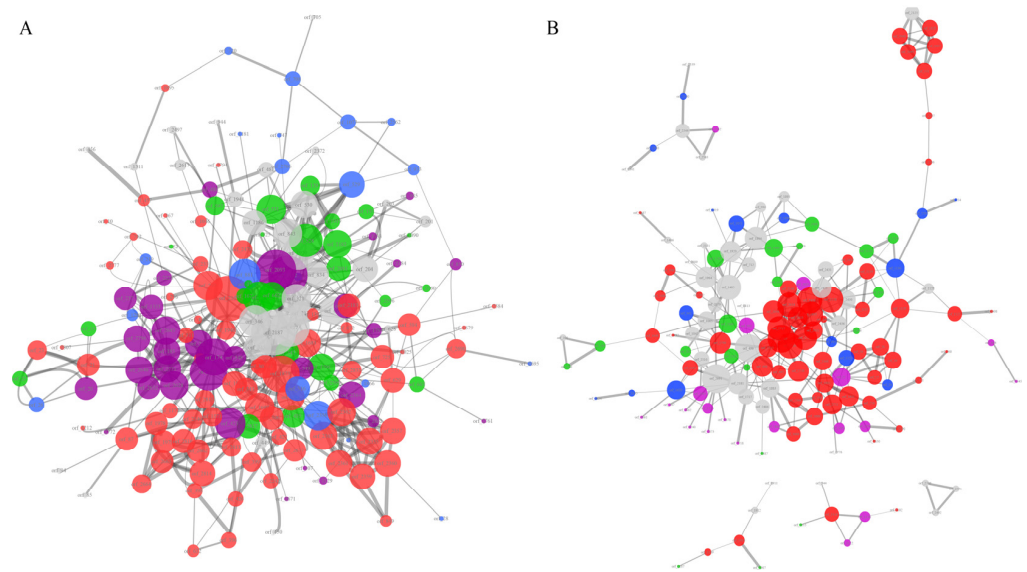


Figure 5. The protein–protein interaction network analysis of unique gene families of the LMO and LVI genomes. The PPI network of LMO (A) referenced to *L. monocytogenes* EGD-e 169963 and the names of the nodes corresponding to Table S3. The PPI network of LMO (B) referenced to *L. ivanovii* 1638 and the names of the nodes corresponding to Table S4. Only those networks with a number of nodes greater than 3 are shown in the graph. The edges of the network represent the relationships of protein–protein interaction, and their line thickness represents the confidence of the relationships between nodes. The size of the nodes represents the degree of the nodes. Different colors of the nodes reflect the different protein function categories: the red represents basic substance transport and metabolism; the purple represents genetic information processing, including replication, transcription, and translation; the blue represents the cellular processes, including cell wall/membrane/envelope biogenesis and cell motility; the green represents the bacteria–environment interaction, including signal transduction, extracellular structures, and defense mechanism; and the grey represents the proteins without meaningful function annotations.

For the UGLVI set, there were 152 proteins shown in the PPI network, with one core network and four small networks (Figure 5B, Table S4). Similar to the UGLMO, most of the proteins in the UGLVI PPI network (68/152, 44.73%) were related to basic substance transport and metabolism, enriched with ABC-type transport systems, PTS transporters, and energy metabolism enzymes. There were 22 (13.16%) proteins related to genetic information processing, including eight DNA-binding transcriptional regulators and six InlC proteins (orf_2796, orf_2507, orf_1673, orf_1678, orf_1682, orf_347), which represent an important factor in the promotion of intercellular invasion [51]. In addition, there were 22 proteins associated with the bacteria–environment interaction, including antibiotic resistance proteins (orf_1153, orf_1180, orf_1480), sensor proteins (orf_1132, orf_1136, orf_1898), and so forth.

For the UGLP gene set, we performed a functional enrichment analysis using the STRING tools. It is interesting to note that the ethanolamine-metabolic-process-related proteins were markedly enriched in the network (60/81, $P_{adj} < 0.001$) (Figure S1, Tables S5 and S6). Ethanolamine is a compound of mammalian cell membranes, and some pathogens can be used as a source of carbon and/or nitrogen. Zeng et. al [68] found that ethanolamine utilization, which is driven by bacterial microcompartments, is essential for the anaerobic growth of LMO. The central genes of the ethanolamine metabolic process are *eutB* and *eutC* (orf_1178 and orf_1179, referenced to *L. monocytogenes* EGD-e 169963; orf_1755 and orf_1754, referenced to *L. ivanovii* 1638), which encode the ethanolamine ammonia-lyase [69]. In addition, five (referenced to *L. monocytogenes* EGD-e 169963) and seven (referenced to *L. ivanovii* 1638) accessory genes related to *eutB* and *eutC* were found in the PPI network [69]. It was found in *L. monocytogenes* that all the *eut* genes were strongly upregulated in the

intestines of infected mice, and the *eut* operon was upregulated during intracellular growth in the cytosol of human colon epithelial cells, but the *eutB*-deleted strains proved to be defective in terms of intracellular growth [70,71]. The upregulation of the *eut* operon was also observed in *L. monocytogenes* that were co-cultured with cheese rind bacteria or grown on vacuum-packed, cold-smoked salmon, which suggests a possible role of the ethanolamine metabolism in the adaptation to stress conditions [72,73]. However, more direct evidence is needed to make clear whether the ability to metabolize ethanolamine contributes to its pathogenicity through a specific mechanism.

As analyzed above, the majority of the unique proteins of *Listeria* pathogens have direct or indirect connections with their pathogenic lifestyle. These unique genes of LMO and LIV are responsible for their differences in niche adaptation and pathogenicity. However, the 33 proteins shown in Figure 5A, 49 proteins in Figure 5B, and 139 proteins in Figure S1 have no explicit function information, which should be studied in the future.

3.1.8. The Distribution of Antibiotics Resistance Genes in the *Listeria* Species

With the use of the generally applied antibiotics, the antibiotic resistance of food-borne strains in many countries has increased [74]. The CARD database was used to investigate the antibiotic resistance gene distribution of the *Listeria* species. As shown in Figure 6, a total of 21 genes exist in the 307 *Listeria* genomes, which belong to 13 drug classes with five resistance mechanisms. The glycopeptide antibiotic resistance genes (*vanTG*, *vanYB*), peptide antibiotic resistance genes (*Lmon_mprF*), phosphonic acid antibiotic resistance genes (*FosX*), and lincosamide antibiotic gene *lin* were the most widely attested antibiotic resistance genes in *Listeria*. LMO, *L. welshimeri*, and *L. innocua* had similar types of antibiotic genes. Importantly, *L. innocua* had the most abundant antibiotic resistance genes, and as many as eight of them were found to exist in the plasmid. These results follow the survey data on antibiotic resistance among *Listeria* [75,76]. The high-level presence of resistance genes in other *Listeria* species, especially *L. innocua*, could increase the possibility of the acquisition of resistance by LMO through horizontal gene transfer in the future.

3.1.9. The Occurrence of Different Types of CRISPR-Cas Systems in *Listeria*

The CRISPR-Cas systems are bacterial-adaptive antiviral immunity systems protecting bacteria from the infection of bacteriophages, which are also associated with the virulence and pathogenicity of pathogens [77,78]. In this study, we investigated the CRISPR-Cas systems of 307 *Listeria* genomes. Five types of CRISPR-Cas systems were found, including I-B, II-A, II-C, III-B, and VI-A, which could be divided into seven sub-types (Table 4). About one-third of the LMO genomes (90/275) had at least one CRISPR-Cas system. Among them, five sub-type CRISPR-Cas systems, except for II-C_n1 and VI-A_n2, were found in it, and I-B_n1 (36.89%) II-A_n1 (49.51%) were the most prevalent subtypes. The subtypes I-B_n2 and III-B_n1 were only detected in the LMO. The subtype II-C_n1 was only detected in LIV, and VI-A_n2 was only detected in *L. seeligeri*. Because of the small numbers of genomes of *L. grayi* and *L. welshimeri*, no CRISPR-Cas system was found in them.

Table 4. The identified types of CRISPR-Cas system in the 307 *Listeria* genomes.

Species	Number of Each Cas-CRISPR System Type							Total
	I-B_n1	I-B_n2	II-A_n1	II-A_n2	II-C_n1	III-B_n1	VI-A_n2	
<i>L. grayi</i>	0	0	0	0	0	0	0	0
<i>L. innocua</i>	0	0	4	0	0	0	0	4
<i>L. ivanovii</i>	2	0	0	2	2	0	0	6
<i>L. marthii</i>	1	0	0	0	0	0	0	1
<i>L. monocytogenes</i>	38	3	51	10	0	1	0	103
<i>L. seeligeri</i>	3	0	1	0	0	0	1	5
<i>L. welshimeri</i>	0	0	0	0	0	0	0	0
Total	44	3	56	12	2	1	1	119

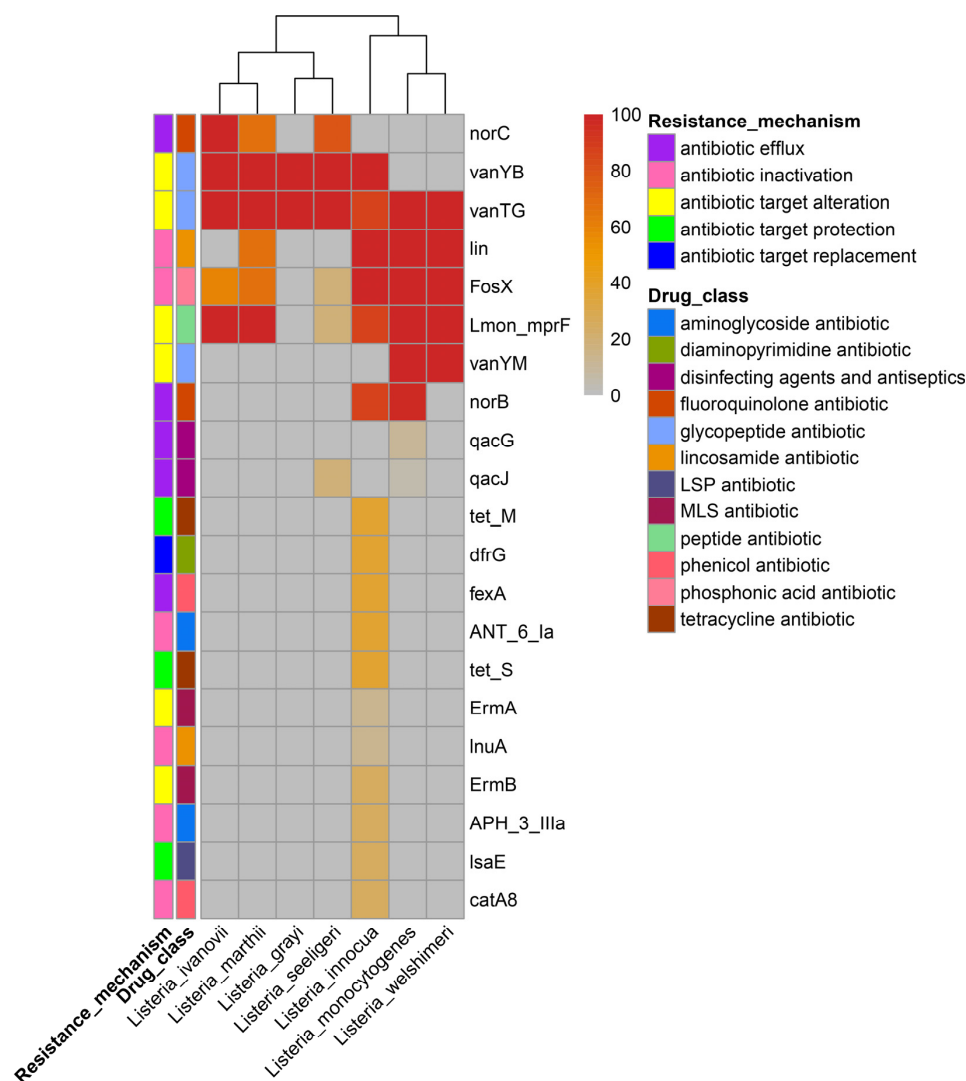


Figure 6. The distribution of antibiotics resistance genes in the *Listeria* species. The percentages of genomes that contain antibiotic resistance genes for each species are shown in the heatmap. The resistance mechanisms of the genes and corresponding drug class are shown in the graph. The LSP antibiotic drug class refers to lincosamide antibiotic, streptogramin antibiotic, and pleuromutilin antibiotic; the MLS refers to macrolide antibiotic, lincosamide antibiotic, and streptogramin antibiotic.

3.1.10. The Characterization of Plasmids from the *Listeria* Species

The plasmid was previously detected in many *Listeria* wildtype strains and is responsible for the transferable antibiotic resistance of LMO [79,80]. A total of 60 plasmids were detected in the 307 *Listeria* genomes, which were classified into 11 types based on the plasmidfinder results (Table 5 and Table S7). The lengths of the plasmids ranged from 2776 bp (CP045971.1) to 152,337 bp (CP022021.1). Nine types of plasmid were found in the LMO, and half of them (26/51) were PLM33. We also investigated the antibiotic resistance genes of the plasmids. The results showed that the plasmids of 15 LMO carried *qacG*/*qacJ* genes, which are related to the resistance of disinfecting agents and antiseptics through the antibiotic efflux mechanism. It is interesting to note that the plasmids of *L. innocua* carried as many as eight resistance genes, including APH(3′)-IIIa, ANT(6)-Ia, ErmB, tet(S), *dfrG*, *catA8*, *InuA*, and *lsaE*, which suggested that there was a risk of drug resistance transmission among the *Listeria* pathogens through horizontal gene transfer. In addition, we did not find any other *Listeria* plasmids carrying antibiotic resistance genes.

Table 5. The plasmid distribution in the 307 *Listeria* genomes.

Species	Number of Each Plasmid Type											Total
	LMIVRS 16815	M640p0 0130	M643p0 0680	pLGU G1	pLI100	pLIS3	pLIS5	pLM33	pLM55 78	pLMIV	pLMUK DL7	
<i>L. grayi</i>	0	0	0	3	0	0	0	0	0	0	0	3
<i>L. innocua</i>	0	2	0	0	1	0	0	2	0	0	0	5
<i>L. monocytogenes</i>	1	6	3	4	0	2	0	26	6	2	1	51
<i>L. seeligeri</i>	0	0	0	0	0	0	1	0	0	0	0	1
Total	1	8	3	7	1	2	1	28	6	2	1	60

3.2. Formatting of Mathematical Components

Core genome size profile model:

$$y = A_1 e^{B_1 x} + C_1 \quad (1)$$

where y is the core genome size; x is the number of the genome; and A_1 , B_1 , and C_1 are free parameters.

Pan-genome size profile model:

$$y = A_2 x^{B_2} + C_2 \quad (2)$$

where y is the pan-genome size; x is the number of the genome; and A_2 , B_2 , and C_2 are free parameters.

4. Conclusions

In this study, we presented a genus-wide comparative genomic study of *Listeria* species to investigate the genetic basis of the phenotypes affecting the pathogenicity and niche adaption of *Listeria* pathogens. The core and pan-genome analysis was performed based on the genomes of LMO, LIV, and NPLS. The core and pan-genome sizes of all the *Listeria* genomes, LMO, LIV, and NPLS were 975/7701, 2060/5382, 2118/3194, and 1203/5308, respectively. The regression of the pan-genome size using the Heaps' law model showed that LMO had an open genome, which can be understood as the genetic basis for its adaption to diverse environments. In addition, the numbers of UGLMO, UGLIV, and UGLP were 204, 242, and 756, respectively. The function annotation results indicated that numerous carbohydrate-metabolism-related proteins for various carbon sources and virulence-associated proteins were included in the unique gene sets, which play important roles in their pathogenicity and niche adaption. Furthermore, the PPI network analysis of UGLMO, UGLIV, and UGLP showed that the majority of these genes were closely connected. Numerous ABC-type transport systems, PTS transporters, and energy metabolism enzymes were clustered in the UGLMO and UGLIV PPI networks, as well as DNA-binding transcriptional regulators, flagella-related proteins, and so on. Interestingly, ethanolamine-metabolic-process-related proteins were significantly enriched in the UGLP network, which might be a significant factor in the pathogenicity of *Listeria* pathogens. However, 33 proteins of UGLMO, 49 proteins of UGLIV, and 139 proteins of UGLP in the PPI network still have no explicit function information, and these proteins might interact with others and should be investigated in the future.

Supplementary Materials: The following supporting information can be downloaded at: <https://www.mdpi.com/article/10.3390/pathogens11121430/s1>, Supplementary Figure S1. Figure S1: The protein–protein interaction network analysis of UGLP. Supplementary Tables S1–S6. Table S1: Genomic details of *Listeria* strains used in the present study. Table S2: The ratio of homologous proteome between genomes. Table S3: Unique genes of LMO referenced to *L. monocytogenes* EGD-e_169963. Table S4: Unique genes of LMO referenced to *L. ivanovii* 1638. Table S5: Unique genes of *Listeria* pathogens (UGLP) referenced to *L. ivanovii* 1638. Table S6: Unique genes of *Listeria* pathogens

(UGLP) referenced to *L. monocytogenes* EGD-e_169963. Table S7. Characteristics of the plasmids of *Listeria* strains.

Author Contributions: Conceptualization, X.L. and D.C.; data collection and curation, X.Z., Q.L. (Qinqin Long), X.Y. and A.Y.; formal analysis, Q.L. (Qunfeng Lu) and D.C.; methodology, Q.L. (Qunfeng Lu) and D.C.; supervision, X.L. and D.C.; validation, X.Z.; writing—original draft, Q.L. (Qunfeng Lu) and X.Z.; writing—review and editing, D.C. All authors have read and agreed to the published version of the manuscript.

Funding: This research was funded by the Baise Science and Technology Plan Project (baike202236, baike202235), National Natural Science Foundation of China (No. 81860489), the Science-Technology Program of Guangxi (No. AD19245174), Guangxi Training Program for Medical High-level Academic Leaders (No. 6 of Guiweikejiaofa (2020)-15), Bose Talent Highland (No. 2020-3-2), and the Natural Science Foundation of YMU (No. yy2020ky021).

Institutional Review Board Statement: Not applicable.

Informed Consent Statement: Not applicable.

Data Availability Statement: The data used to support the findings of this study are available from the corresponding author upon request.

Conflicts of Interest: The authors declare no conflict of interest.

References

- Batt, C.A. *LISTERIA* | Introduction. In *Encyclopedia of Food Microbiology*, 2nd ed.; Batt, C.A., Tortorello, M.L., Eds.; Academic Press: Oxford, UK, 2014; pp. 466–469.
- Conly, J.M.; Johnston, B.L. *Listeria*: A persistent food-borne pathogen. *Can. J. Infect. Dis. Med. Microbiol.* **2008**, *19*, 327–328. [[CrossRef](#)] [[PubMed](#)]
- Hafner, L.; Pichon, M.; Burucoa, C.; Nusser, S.H.A.; Moura, A.; Garcia-Garcera, M.; Lecuit, M. *Listeria monocytogenes* faecal carriage is common and depends on the gut microbiota. *Nat. Commun.* **2021**, *12*, 6826. [[CrossRef](#)] [[PubMed](#)]
- Kreft, J.; Vázquez-Boland, J.A.; Altrock, S.; Dominguez-Bernal, G.; Goebel, W. Pathogenicity islands and other virulence elements in *Listeria*. *Curr. Top. Microbiol. Immunol.* **2002**, *264*, 109–125. [[PubMed](#)]
- Radoshevich, L.; Cossart, P. *Listeria monocytogenes*: Towards a complete picture of its physiology and pathogenesis. *Nat. Rev. Microbiol.* **2018**, *16*, 32–46. [[CrossRef](#)]
- Cossart, P.; Vicente, M.F.; Mengaud, J.; Baquero, F.; Perez-Diaz, J.C.; Berche, P. Listeriolysin O is essential for virulence of *Listeria monocytogenes*: Direct evidence obtained by gene complementation. *Infect. Immun.* **1989**, *57*, 3629–3636. [[CrossRef](#)] [[PubMed](#)]
- Smith, G.A.; Marquis, H.; Jones, S.; Johnston, N.C.; Portnoy, D.A.; Goldfine, H. The two distinct phospholipases C of *Listeria monocytogenes* have overlapping roles in escape from a vacuole and cell-to-cell spread. *Infect. Immun.* **1995**, *63*, 4231–4237. [[CrossRef](#)]
- Vega, Y.; Dickneite, C.; Ripio, M.T.; Böckmann, R.; González-Zorn, B.; Novella, S.; Domínguez-Bernal, G.; Goebel, W.; Vázquez-Boland, J.A. Functional similarities between the *Listeria monocytogenes* virulence regulator PrfA and cyclic AMP receptor protein: The PrfA* (Gly145Ser) mutation increases binding affinity for target DNA. *J. Bacteriol.* **1998**, *180*, 6655–6660. [[CrossRef](#)] [[PubMed](#)]
- Mitchell, G.; Ge, L.; Huang, Q.; Chen, C.; Kianian, S.; Roberts, M.F.; Schekman, R.; Portnoy, D.A. Avoidance of autophagy mediated by PlcA or ActA is required for *Listeria monocytogenes* growth in macrophages. *Infect. Immun.* **2015**, *83*, 2175–2184. [[CrossRef](#)] [[PubMed](#)]
- Alvarez, D.E.; Agaisse, H. The Metalloprotease Mpl Supports *Listeria monocytogenes* Dissemination through Resolution of Membrane Protrusions into Vacuoles. *Infect. Immun.* **2016**, *84*, 1806–1814. [[CrossRef](#)] [[PubMed](#)]
- Hyatt, D.; Chen, G.-L.; Locascio, P.F.; Land, M.L.; Larimer, F.W.; Hauser, L.J. Prodigal: Prokaryotic gene recognition and translation initiation site identification. *BMC Bioinform.* **2010**, *11*, 119. [[CrossRef](#)]
- Lagesen, K.; Hallin, P.; Rødland, E.A.; Staerfeldt, H.H.; Rognes, T.; Ussery, D.W. RNAMmer: Consistent and rapid annotation of ribosomal RNA genes. *Nucleic Acids Res.* **2007**, *35*, 3100–3108. [[CrossRef](#)]
- Lowe, T.M.; Eddy, S.R. tRNAscan-SE: A program for improved detection of transfer RNA genes in genomic sequence. *Nucleic Acids Res.* **1997**, *25*, 955–964. [[CrossRef](#)] [[PubMed](#)]
- Carattoli, A.; Hasman, H. PlasmidFinder and In Silico pMLST: Identification and Typing of Plasmid Replicons in Whole-Genome Sequencing (WGS). *Methods Mol. Biol.* **2020**, *2075*, 285–294. [[CrossRef](#)] [[PubMed](#)]
- Schmartz, G.P.; Hartung, A.; Hirsch, P.; Kern, F.; Fehlmann, T.; Müller, R.; Keller, A. PLSDB: Advancing a comprehensive database of bacterial plasmids. *Nucleic Acids Res.* **2022**, *50*, D273–D278. [[CrossRef](#)] [[PubMed](#)]
- Fu, L.; Niu, B.; Zhu, Z.; Wu, S.; Li, W. CD-HIT: Accelerated for clustering the next-generation sequencing data. *Bioinformatics* **2012**, *28*, 3150–3152. [[CrossRef](#)] [[PubMed](#)]

17. Li, L.; Stoeckert, C.J.; Roos, D.S. OrthoMCL: Identification of ortholog groups for eukaryotic genomes. *Genome Res.* **2003**, *13*, 2178–2189. [[CrossRef](#)]
18. Dongen, S. *A Cluster Algorithm for Graphs*; Centrum Wiskunde & Informatica (CWI): The National Research Institute for Mathematics and Computer Science in the Netherlands: Amsterdam, The Netherlands, 2000; pp. 1–40.
19. Katoh, K.; Standley, D.M. MAFFT multiple sequence alignment software version 7: Improvements in performance and usability. *Mol. Biol. Evol.* **2013**, *30*, 772–780. [[CrossRef](#)]
20. Castresana, J. Selection of Conserved Blocks from Multiple Alignments for Their Use in Phylogenetic Analysis. *Mol. Biol. Evol.* **2000**, *17*, 540–552. [[CrossRef](#)]
21. Stamatakis, A. RAxML version 8: A tool for phylogenetic analysis and post-analysis of large phylogenies. *Bioinformatics* **2014**, *30*, 1312–1313. [[CrossRef](#)]
22. Letunic, I.; Bork, P. Interactive Tree of Life (iTOL) v5: An online tool for phylogenetic tree display and annotation. *Nucleic Acids Res.* **2021**, *49*, W293–W296. [[CrossRef](#)]
23. Huerta-Cepas, J.; Szklarczyk, D.; Heller, D.; Hernandez-Plaza, A.; Forslund, S.K.; Cook, H.; Mende, D.R.; Letunic, I.; Rattei, T.; Jensen, L.J.; et al. eggNOG 5.0: A hierarchical, functionally and phylogenetically annotated orthology resource based on 5090 organisms and 2502 viruses. *Nucleic Acids Res.* **2019**, *47*, D309–D314. [[CrossRef](#)] [[PubMed](#)]
24. Galperin, M.Y.; Wolf, Y.I.; Makarova, K.S.; Vera Alvarez, R.; Landsman, D.; Koonin, E.V. COG database update: Focus on microbial diversity, model organisms, and widespread pathogens. *Nucleic Acids Res.* **2021**, *49*, D274–D281. [[CrossRef](#)] [[PubMed](#)]
25. Finn, R.D.; Attwood, T.K.; Babbitt, P.C.; Bateman, A.; Bork, P.; Bridge, A.; Chang, H.Y.; Dosztanyi, Z.; Elgebal, S.; Fraser, M. InterPro in 2017—Beyond protein family and domain annotations. *Nucleic Acids Res.* **2017**, *45*, D190–D199. [[CrossRef](#)]
26. Chen, L.; Zheng, D.; Liu, B.; Yang, J.; Jin, Q. VFDB 2016: Hierarchical and refined dataset for big data analysis—10 years on. *Nucleic Acids Res.* **2016**, *44*, D694–D697. [[CrossRef](#)] [[PubMed](#)]
27. Chen, H.; Boutros, P.C. VennDiagram: A package for the generation of highly-customizable Venn and Euler diagrams in R. *BMC Bioinform.* **2011**, *12*, 35. [[CrossRef](#)] [[PubMed](#)]
28. Szklarczyk, D.; Franceschini, A.; Wyder, S.; Forslund, K.; Heller, D.; Huertacepas, J.; Simonovic, M.; Roth, A.; Santos, A.; Tsafou, K.P. STRING v10: Protein-protein interaction networks, integrated over the tree of life. *Nucleic Acids Res.* **2015**, *43*, 87–105. [[CrossRef](#)]
29. Shannon, P.; Markiel, A.; Ozier, O.; Baliga, N.S.; Wang, J.T.; Ramage, D.; Amin, N.; Schwikowski, B.; Ideker, T. Cytoscape: A Software Environment for Integrated Models of Biomolecular Interaction Networks. *Genome Res.* **2003**, *13*, 2498–2504. [[CrossRef](#)]
30. Alcock, B.P.; Raphenya, A.R.; Lau, T.T.Y.; Tsang, K.K.; Bouchard, M.; Edalatmand, A.; Huynh, W.; Nguyen, A.V.; Cheng, A.A.; Liu, S.; et al. CARD 2020: Antibiotic resistance surveillance with the comprehensive antibiotic resistance database. *Nucleic Acids Res.* **2020**, *48*, D517–D525. [[CrossRef](#)]
31. Grissa, I.; Vergnaud, G.; Pourcel, C. CRISPRFinder: A web tool to identify clustered regularly interspaced short palindromic repeats. *Nucleic Acids Res.* **2007**, *35*, W52–W57. [[CrossRef](#)]
32. Glaser, P.; Frangeul, L.; Buchrieser, C.; Rusniok, C.; Amend, A.; Baquero, F.; Berche, P.; Bloecker, H.; Brandt, P.; Chakraborty, T.; et al. Comparative genomics of *Listeria* species. *Science* **2001**, *294*, 849–852. [[CrossRef](#)]
33. Baroncelli, R.; Amby, D.B.; Zapparata, A.; Sarrocco, S.; Vannacci, G.; Le Floch, G.; Harrison, R.J.; Holub, E.; Sukno, S.A.; Sreenivasaprasad, S.; et al. Gene family expansions and contractions are associated with host range in plant pathogens of the genus *Colletotrichum*. *BMC Genom.* **2016**, *17*, 555. [[CrossRef](#)] [[PubMed](#)]
34. Schmid, M.W.; Ng, E.Y.W.; Lampidis, R.; Emmerth, M.; Walcher, M.; Kreft, J.; Goebel, W.; Wagner, M.; Schleifer, K.-H. Evolutionary history of the genus *Listeria* and its virulence genes. *Syst. Appl. Microbiol.* **2005**, *28*, 1–18. [[CrossRef](#)]
35. Boerlin, P.; Rocourt, J.; Piffaretti, J.C. Taxonomy of the genus *Listeria* by using multilocus enzyme electrophoresis. *Int. J. Syst. Bacteriol.* **1991**, *41*, 59–64. [[CrossRef](#)]
36. Tettelin, H.; Riley, D.; Cattuto, C.; Medini, D. Comparative genomics: The bacterial pan-genome. *Curr. Opin. Microbiol.* **2008**, *11*, 472–477. [[CrossRef](#)]
37. Medini, D.; Donati, C.; Tettelin, H.; Massignani, V.; Rappuoli, R. The microbial pan-genome. *Curr. Opin. Genet. Dev.* **2005**, *15*, 589–594. [[CrossRef](#)]
38. Lefebure, T.; Stanhope, M.J. Evolution of the core and pan-genome of *Streptococcus*: Positive selection, recombination, and genome composition. *Genome Biol.* **2007**, *8*, R71. [[CrossRef](#)]
39. Siefert, J.L. Defining the Mobilome. In *Horizontal Gene Transfer: Genomes in Flux*; Gogarten, M.B., Gogarten, J.P., Olendzenski, L.C., Eds.; Humana Press: Totowa, NJ, USA, 2009; pp. 13–27.
40. Muchaamba, F.; Eshwar, A.; Stevens, M.; von Ah, U.; Tasara, T. Variable Carbon Source Utilization, Stress Resistance, and Virulence Profiles Among *Listeria monocytogenes* Strains Responsible for Listeriosis Outbreaks in Switzerland. *Front. Microbiol.* **2019**, *10*, 957. [[CrossRef](#)]
41. Deutscher, J.; Aké, F.; Zebre, A.; Cao, T.; Kentache, T.; Pham, Q.; Mokhtari, A.; Joyet, P.; Milohanic, E. Carbohydrate Utilization by *Listeria monocytogenes* and its Influence on Virulence Gene Expression. In *Listeria monocytogenes: Food Sources, Prevalence and Management Strategies*; Nova science publishers: Hauppauge, NY, USA, 2014; pp. 49–76.
42. Milenbachs, A.A.; Brown, D.P.; Moors, M.; Youngman, P. Carbon-source regulation of virulence gene expression in *Listeria monocytogenes*. *Mol. Microbiol.* **1997**, *23*, 1075–1085. [[CrossRef](#)]

43. McLaughlin, H.P.; Hill, C.; Gahan, C.G.M. The impact of iron on *Listeria monocytogenes*; inside and outside the host. *Curr. Opin. Biotechnol.* **2011**, *22*, 194–199. [[CrossRef](#)]
44. Orelle, C.; Mathieu, K.; Jault, J.-M. Multidrug ABC transporters in bacteria. *Res. Microbiol.* **2019**, *170*, 381–391. [[CrossRef](#)]
45. Rea, R.B.; Gahan, C.G.M.; Hill, C. Disruption of Putative Regulatory Loci in *Listeria monocytogenes* Demonstrates a Significant Role for Fur and PerR in Virulence. *Infect. Immun.* **2004**, *72*, 717–727. [[CrossRef](#)] [[PubMed](#)]
46. Ledala, N.; Sengupta, M.; Muthaiyan, A.; Wilkinson, B.J.; Jayaswal, R.K. Transcriptomic response of *Listeria monocytogenes* to iron limitation and Fur mutation. *Appl. Environ. Microbiol.* **2010**, *76*, 406–416. [[CrossRef](#)] [[PubMed](#)]
47. Lebreton, A.; Cossart, P. RNA- and protein-mediated control of *Listeria monocytogenes* virulence gene expression. *RNA Biol.* **2017**, *14*, 460–470. [[CrossRef](#)] [[PubMed](#)]
48. Boujemaa-Paterski, R.; Gouin, E.; Hansen, G.; Samarín, S.; Le Clainche, C.; Didry, D.; Dehoux, P.; Cossart, P.; Kocks, C.; Carlier, M.-F.; et al. *Listeria* Protein ActA Mimics WASP Family Proteins: It Activates Filament Barbed End Branching by Arp2/3 Complex. *Biochemistry* **2001**, *40*, 11390–11404. [[CrossRef](#)]
49. Cabanes, D.; Dussurget, O.; Dehoux, P.; Cossart, P. Auto, a surface associated autolysin of *Listeria monocytogenes* required for entry into eukaryotic cells and virulence. *Mol. Microbiol.* **2004**, *51*, 1601–1614. [[CrossRef](#)] [[PubMed](#)]
50. Gouin, E.; Adib-Conquy, M.; Balestrino, D.; Nahori, M.-A.; Villiers, V.; Colland, F.; Dramsi, S.; Dussurget, O.; Cossart, P. The *Listeria monocytogenes* InlC protein interferes with innate immune responses by targeting the I κ B kinase subunit IKK α . *Proc. Natl. Acad. Sci. USA* **2010**, *107*, 17333–17338. [[CrossRef](#)]
51. Rajabian, T.; Gavicherla, B.; Heisig, M.; Müller-Altrock, S.; Goebel, W.; Gray-Owen, S.D.; Ireton, K. The bacterial virulence factor InlC perturbs apical cell junctions and promotes cell-to-cell spread of *Listeria*. *Nat. Cell Biol.* **2009**, *11*, 1212–1218. [[CrossRef](#)]
52. Chico-Calero, I.; Suárez, M.; González-Zorn, B.; Scotti, M.; Slaghuis, J.; Goebel, W.; Vázquez-Boland, J.A. Hpt, a bacterial homolog of the microsomal glucose-6-phosphate translocase, mediates rapid intracellular proliferation in *Listeria*. *Proc. Natl. Acad. Sci. USA* **2002**, *99*, 431–436. [[CrossRef](#)]
53. González-Zorn, B.; Domínguez-Bernal, G.; Suárez, M.; Ripio, M.T.; Vega, Y.; Novella, S.; Vázquez-Boland, J.A. The smcL gene of *Listeria ivanovii* encodes a sphingomyelinase C that mediates bacterial escape from the phagocytic vacuole. *Mol. Microbiol.* **1999**, *33*, 510–523. [[CrossRef](#)]
54. Mengaud, J.; Ohayon, H.; Gounon, P.; Mège, R.-M.; Cossart, P. E-Cadherin Is the Receptor for Internalin, a Surface Protein Required for Entry of *L. monocytogenes* into Epithelial Cells. *Cell* **1996**, *84*, 923–932. [[CrossRef](#)] [[PubMed](#)]
55. Asano, K.; Sashinami, H.; Osanai, A.; Asano, Y.; Nakane, A. Autolysin amidase of *Listeria monocytogenes* promotes efficient colonization of mouse hepatocytes and enhances host immune response. *Int. J. Med. Microbiol.* **2011**, *301*, 480–487. [[CrossRef](#)] [[PubMed](#)]
56. Asano, K.; Kakizaki, I.; Nakane, A. Interaction of *Listeria monocytogenes* autolysin amidase with glycosaminoglycans promotes *listerial* adhesion to mouse hepatocytes. *Biochimie* **2012**, *94*, 1291–1299. [[CrossRef](#)] [[PubMed](#)]
57. Ghosh, P.; Halvorsen, E.M.; Ammendolia, D.A.; Mor-Vaknin, N.; O’Riordan, M.X.D.; Brumell, J.H.; Markovitz, D.M.; Higgins, D.E. Invasion of the Brain by *Listeria monocytogenes* Is Mediated by InlF and Host Cell Vimentin. *mBio* **2018**, *9*, e00160-18. [[CrossRef](#)] [[PubMed](#)]
58. Malmirchegini, G.R.; Sjødt, M.; Shnitkind, S.; Sawaya, M.R.; Rosinski, J.; Newton, S.M.; Klebba, P.E.; Clubb, R.T. Novel Mechanism of Hemin Capture by Hbp2, the Hemoglobin-binding Hemophore from *Listeria monocytogenes*. *J. Biol. Chem.* **2014**, *289*, 34886–34899. [[CrossRef](#)]
59. Borezée, E.; Pellegrini, E.; Beretti, J.-L.; Berche, P. SvpA, a novel surface virulence-associated protein required for intracellular survival of *Listeria monocytogenes*. *Microbiology* **2001**, *147*, 2913–2923. [[CrossRef](#)]
60. Goldfine, H.; Knob, C.; Alford, D.; Bentz, J. Membrane permeabilization by *Listeria monocytogenes* phosphatidylinositol-specific phospholipase C is independent of phospholipid hydrolysis and cooperative with listeriolysin O. *Proc. Natl. Acad. Sci. USA* **1995**, *92*, 2979–2983. [[CrossRef](#)]
61. Vázquez-Boland, J.A.; Kuhn, M.; Berche, P.; Chakraborty, T.; Domínguez-Bernal, G.; Goebel, W.; González-Zorn, B.; Wehland, J.; Kreft, J. *Listeria* pathogenesis and molecular virulence determinants. *Clin. Microbiol. Rev.* **2001**, *14*, 584–640. [[CrossRef](#)]
62. Poyart, C.; Abachin, E.; Razafimanantsoa, I.; Berche, P. The zinc metalloprotease of *Listeria monocytogenes* is required for maturation of phosphatidylcholine phospholipase C: Direct evidence obtained by gene complementation. *Infect. Immun.* **1993**, *61*, 1576–1580. [[CrossRef](#)]
63. Forster, B.M.; Zemansky, J.; Portnoy, D.A.; Marquis, H. Posttranslocation chaperone PrsA2 regulates the maturation and secretion of *Listeria monocytogenes* proprotein virulence factors. *J. Bacteriol.* **2011**, *193*, 5961–5970. [[CrossRef](#)]
64. Cheng, Y.; Promadej, N.; Kim, J.W.; Kathariou, S. Teichoic acid glycosylation mediated by gtcA is required for phage adsorption and susceptibility of *Listeria monocytogenes* serotype 4b. *Appl. Environ. Microbiol.* **2008**, *74*, 1653–1655. [[CrossRef](#)]
65. Alves, J.A.; Previato-Mello, M.; Barroso, K.C.M.; Koide, T.; da Silva Neto, J.F. The MarR family regulator OsbR controls oxidative stress response, anaerobic nitrate respiration, and biofilm formation in *Chromobacterium violaceum*. *BMC Microbiol.* **2021**, *21*, 304. [[CrossRef](#)] [[PubMed](#)]
66. O’Neil, H.S.; Marquis, H. *Listeria monocytogenes* flagella are used for motility, not as adhesins, to increase host cell invasion. *Infect. Immun.* **2006**, *74*, 6675–6681. [[CrossRef](#)] [[PubMed](#)]
67. Lemon, K.P.; Higgins, D.E.; Kolter, R. Flagellar motility is critical for *Listeria monocytogenes* biofilm formation. *J. Bacteriol.* **2007**, *189*, 4418–4424. [[CrossRef](#)] [[PubMed](#)]

68. Zeng, Z.; Boeren, S.; Bhandula, V.; Light, S.H.; Smid, E.J.; Notebaart, R.A.; Abee, T. Bacterial Microcompartments Coupled with Extracellular Electron Transfer Drive the Anaerobic Utilization of Ethanolamine in *Listeria monocytogenes*. *mSystems* **2021**, *6*, e01349-20. [[CrossRef](#)] [[PubMed](#)]
69. Garsin, D.A. Ethanolamine utilization in bacterial pathogens: Roles and regulation. *Nat. Rev. Microbiol.* **2010**, *8*, 290–295. [[CrossRef](#)]
70. Joseph, B.; Przybilla, K.; Stühler, C.; Schauer, K.; Slaghuis, J.; Fuchs, T.M.; Goebel, W. Identification of *Listeria monocytogenes* genes contributing to intracellular replication by expression profiling and mutant screening. *J. Bacteriol.* **2006**, *188*, 556–568. [[CrossRef](#)]
71. Toledoarana, A.; Dussurget, O.; Nikitas, G.; Sesto, N.; Guetrevillet, H.; Balestrino, D.; Loh, E.; Gripenland, J.; Tiensuu, T.; Vaitkevicius, K. The *Listeria* transcriptional landscape from saprophytism to virulence. *Nature* **2009**, *459*, 950–956. [[CrossRef](#)]
72. Anast, J.M.; Schmitz-Esser, S. The transcriptome of *Listeria monocytogenes* during co-cultivation with cheese rind bacteria suggests adaptation by induction of ethanolamine and 1,2-propanediol catabolism pathway genes. *PLoS ONE* **2020**, *15*, e0233945. [[CrossRef](#)]
73. Tang, S.; Orsi, R.H.; den Bakker, H.C.; Wiedmann, M.; Boor, K.J.; Bergholz, T.M. Transcriptomic Analysis of the Adaptation of *Listeria monocytogenes* to Growth on Vacuum-Packed Cold Smoked Salmon. *Appl. Environ. Microbiol.* **2015**, *81*, 6812–6824. [[CrossRef](#)]
74. Olaimat, A.N.; Al-Holy, M.A.; Shahbaz, H.M.; Al-Nabulsi, A.A.; Abu Ghoush, M.H.; Osaili, T.M.; Ayyash, M.M.; Holley, R.A. Emergence of Antibiotic Resistance in *Listeria monocytogenes* Isolated from Food Products: A Comprehensive Review. *Compr Rev Food Sci Food Saf* **2018**, *17*, 1277–1292. [[CrossRef](#)]
75. Walsh, D.; Duffy, G.; Sheridan, J.J.; Blair, I.S.; McDowell, D.A. Antibiotic resistance among *Listeria*, including *Listeria monocytogenes*, in retail foods. *J. Appl. Microbiol.* **2001**, *90*, 517–522. [[CrossRef](#)] [[PubMed](#)]
76. Charpentier, E.; Gerbaud, G.; Jacquet, C.; Rocourt, J.; Courvalin, P. Incidence of antibiotic resistance in *Listeria* species. *J. Infect. Dis.* **1995**, *172*, 277–281. [[CrossRef](#)] [[PubMed](#)]
77. Louwen, R.; Staals, R.H.; Endtz, H.P.; van Baarlen, P.; van der Oost, J. The role of CRISPR-Cas systems in virulence of pathogenic bacteria. *Microbiol. Mol. Biol. Rev.* **2014**, *78*, 74–88. [[CrossRef](#)] [[PubMed](#)]
78. Sampson, T.R.; Napier, B.A.; Schroeder, M.R.; Louwen, R.; Zhao, J.; Chin, C.Y.; Ratner, H.K.; Llewellyn, A.C.; Jones, C.L.; Laroui, H.; et al. A CRISPR-Cas system enhances envelope integrity mediating antibiotic resistance and inflammasome evasion. *Proc. Natl. Acad. Sci. USA* **2014**, *111*, 11163–11168. [[CrossRef](#)]
79. Poyart-Salmeron, C.; Carlier, C.; Trieu-Cuot, P.; Courtieu, A.L.; Courvalin, P. Transferable plasmid-mediated antibiotic resistance in *Listeria monocytogenes*. *Lancet* **1990**, *335*, 1422–1426. [[CrossRef](#)]
80. Chmielowska, C.; Korsak, D.; Chapkauskaitse, E.; Decewicz, P.; Lasek, R.; Szuplewska, M.; Bartosik, D. Plasmidome of *Listeria* spp.-The repA-Family Business. *Int. J. Mol. Sci.* **2021**, *22*, 10320. [[CrossRef](#)]